

# Numerical experiments to elucidate propagation effects in high harmonic generation from solids

YAMADA Shunsuke

Ultrafast Dynamics Group, Department of Advanced Photon Research



Recently, high-order harmonic generation (HHG) in solids has been the subject of extensive experimental and theoretical research. HHG in waves reflected or transmitted from a solid thin film is thought to be significantly modulated by the nonlinear light-propagation effect within the thin film [1]. However, it is impossible to experimentally observe this modulation inside thin films. First-principles calculations using the time-dependent density functional theory (TDDFT) can provide realistic and reliable descriptions for the microscopic mechanisms underlying HHG in solids [2]. In this study [3], numerical experiments were conducted to investigate the nonlinear light-propagation effect in HHG from laser-irradiated silicon (Si) thin films by employing a computational method that combines Maxwell's equations for light propagation and TDDFT for electron dynamics.

We consider the irradiation of a free-standing Si thin film of thickness  $d$  in vacuum by an ultrashort light pulse of a linearly polarized plane wave with normal incidence [Fig. 1(a)]. The light propagation is described in the macroscopic scale by solving the following one-dimensional wave equation:

$$\left(\frac{1}{c^2} \frac{\partial^2}{\partial t^2} - \frac{\partial^2}{\partial z^2}\right) \mathbf{A}_Z(t) = \frac{4\pi}{c} \mathbf{J}_Z(t),$$

where  $Z$  is the macroscopic coordinate.  $\mathbf{A}_Z(t)$  and  $\mathbf{J}_Z(t)$  are the vector potential and current density, respectively, of the film. This wave equation is solved using a one-dimensional grid for the  $Z$  variable. At each grid point of  $Z$  inside the film, we consider an infinite crystalline system of the film material. The electronic motion in the unit cell of each crystalline system is described by the Bloch orbitals  $u_{nk,z}(\mathbf{r}, t)$ , which satisfy the time-dependent Kohn–Sham equation:

$$i\hbar \frac{\partial}{\partial t} u_{nk,z}(\mathbf{r}, t) = h_{\mathbf{k}}[\mathbf{A}_Z](t) u_{nk,z}(\mathbf{r}, t),$$

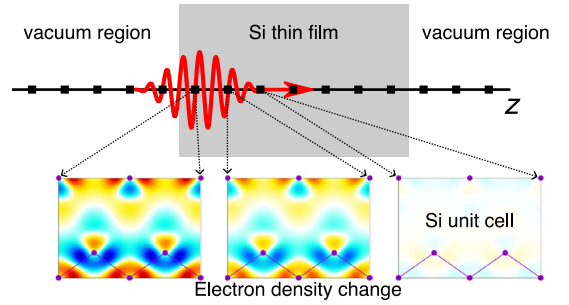
where  $h_{\mathbf{k}}[\mathbf{A}_Z](t) = (1/2m)(-i\hbar\nabla + \hbar\mathbf{k} + (e/c)\mathbf{A}_Z(t))^2 + V_{\text{KS}}(\mathbf{r}, t)$  is the effective single-electron Hamiltonian and  $V_{\text{KS}}(\mathbf{r}, t)$  is the Kohn–Sham potential. The electric current density averaged over the unit-cell volume  $\Omega$  is defined as follows:

$$\mathbf{J}_Z(t) = -e \int_{\Omega} \frac{d^3r}{N_k \Omega} \sum_{n,k} u_{nk,z}^*(\mathbf{r}, t) \left[ \frac{\mathbf{r}}{i}, h_{\mathbf{k}}[\mathbf{A}_Z](t) \right] u_{nk,z}(\mathbf{r}, t).$$

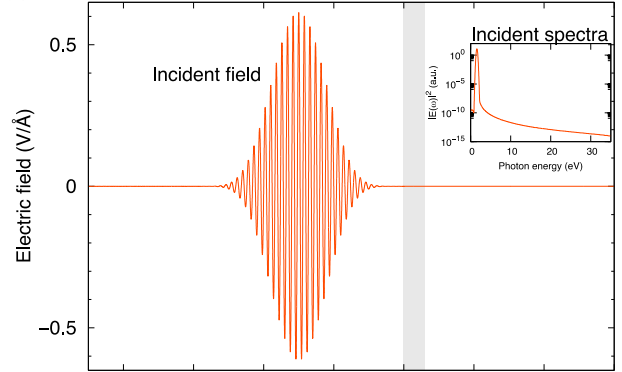
By simultaneously solving the above equations, the ultrafast and nonlinear dynamics of the light pulse and electrons inside the film can be simulated. We call this method [4] “multiscale Maxwell-TDDFT.”

Figures 1(b) and (c) show snapshots of the electric field of the light pulse propagating through a thin Si film with a thickness  $d = 3000$  nm. Figure 1(b) presents the electric field of the initial pulse ( $t = 0$  fs), which is located in front of the film, wherein the film is presented as a thin gray area. We used an incident pulse with a wavelength of 800 nm, full-width-at-half-maximum (FWHM) of 21.4 fs, and peak intensity of  $5 \times 10^{12}$  W/cm<sup>2</sup>. Figure 1(c) shows a snapshot of the electric field at  $t = 150$  fs. Here, we display the results corresponding to initial pulses of two different maximum intensities: a strong pulse ( $I = 5 \times 10^{12}$  W/cm<sup>2</sup>, red solid line), and a weak pulse ( $I = 10^9$  W/cm<sup>2</sup>, blue dotted line). Linear

(a) Multiscale Maxwell-TDDFT method



(b)  $t = 0$  fs



(c)  $t = 150$  fs

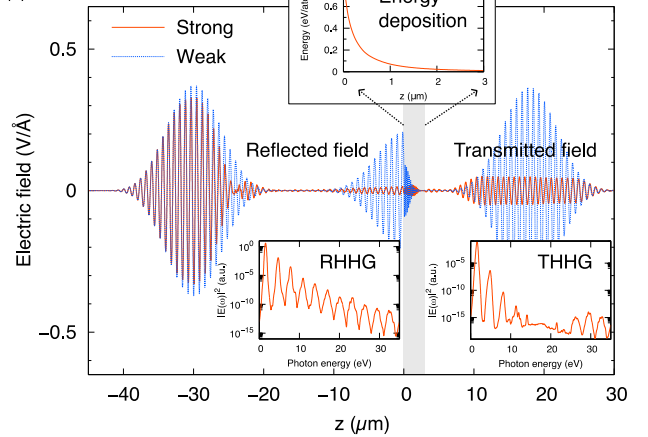


Fig. 1 (a) Overview of the multiscale Maxwell-TDDFT method for light propagation through a thin Si film. The electron density changes driven by the light pulse are illustrated for the first three grid points. (b) Electric field at  $t = 0$ . The incident pulse is generated in front of the thin Si film, which is exhibited as a gray area. (c) Electric field at  $t = 150$  fs is shown for the case of two incident pulses: a strong pulse ( $I = 5 \times 10^{12}$  W/cm<sup>2</sup>, red solid line) and a weak pulse ( $I = 10^9$  W/cm<sup>2</sup>, blue dotted line) scaled up by a factor of  $\sqrt{5000}$ . The Fourier spectra of the respective pulses and energy deposition [(c)] are shown in the insets.

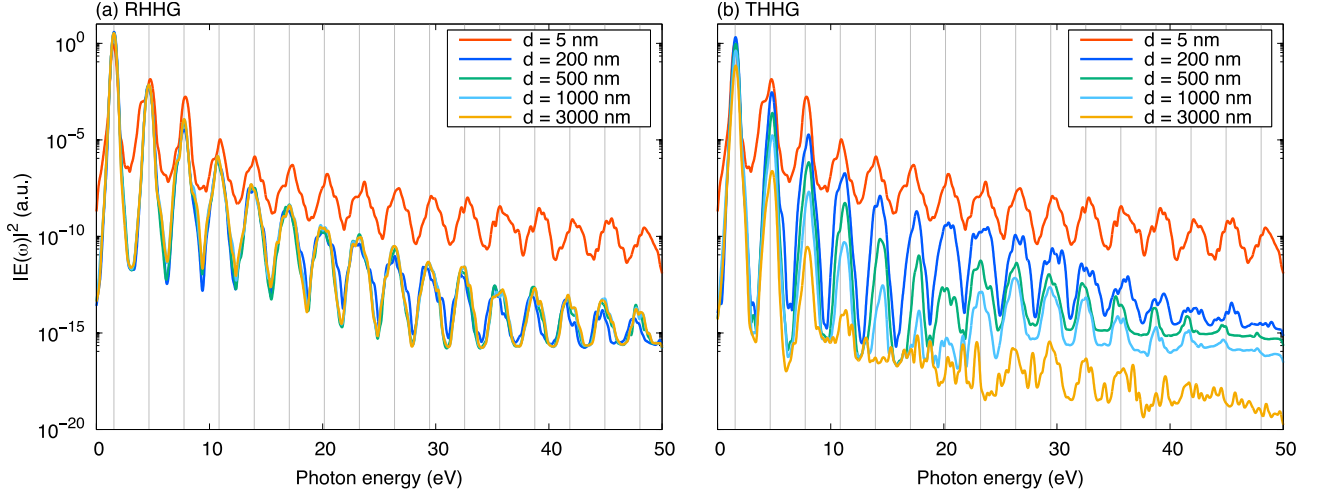


Fig. 2 HHG spectra for the waves (a) reflected and (b) transmitted from the thin Si film with a thickness of  $d = 5, 200, 500, 1000,$  and  $3000$  nm.

propagation is expected for the weak pulses. In the figure, the weak pulse is multiplied by a factor of  $\sqrt{5000}$  so that the differences between the two lines manifest nonlinear effects in the stronger pulse. The reflected and transmitted pulses are shown in Figure 1(c). They are separated from the film (left for the reflected pulses and right for the transmitted pulses). There also appears to be a component around the film, which is caused by reflection at the back surface of the film. By Fourier transforming the reflected and transmitted fields, we obtain the HHG spectra for the respective fields, as depicted in the insets.

Figure 2 shows the calculated HHG spectra in the waves reflected and transmitted from thin Si films with thicknesses of  $d = 5, 200, 500, 1000,$  and  $3000$  nm. We used an incident pulse with a wavelength of  $800$  nm, FWHM of  $21.4$  fs, and peak intensity of  $4 \times 10^{12}$  W/cm<sup>2</sup>. The spectra for reflection and transmission, for a film thickness of  $5$  nm, are equivalent and are the strongest among the signals of films of different thicknesses. These features have already been reported in our previous analysis [5], and can be understood in terms of the two-dimensional approximation for electromagnetism, which is valid for very thin films. While the reflection HHG [Fig. 2(a)] is almost saturated at  $d = 200$  nm, the transmission HHG [Fig. 2(b)] continuously decreases as the thickness increases. In particular, the latter for  $d = 1000$  nm shows a dip around the photon energy of  $20$  eV. Through frequency- and depth-resolved analyses of light pulses, we find that the transmission HHG has two origins: the HHG generated near the front edge and propagating to the back surface, and that generated near the back edge and emitted directly [3]. The dominant mechanism of the transmission of HHG is found to depend on the thickness of the thin film and the frequency of the HHG. For the film with  $d = 1000$  nm, a transmission HHG with a frequency below  $20$  eV is generated near the back edge, whereas that with a frequency above  $20$  eV is generated near the front edge and propagates from there to the back surface. The transmission

HHGs below and above  $20$  eV have different origins, and the dip at  $20$  eV is due to the combination of the two mechanisms.

In this study, we found that the nonlinear propagation dynamics of light pulses cause significant effects in HHG from nano to micrometer-thick Si films. This study demonstrates that the multiscale Maxwell-TDDFT scheme provides a reliable description of such phenomena.

## Acknowledgments

The authors thank T. Otobe, D. Freeman, A. Kheifets, and K. Yabana. This research was supported by JST-CREST under grant number JP-MJCR16N5, MEXT Quantum Leap Flagship Program (MEXT Q-LEAP) Grant Number JPMXS0118068681 and JPMXS0118067246, and JSPS KAKENHI Grant Number 20H2649. Calculations were carried out on the Fugaku supercomputer with the support of the HPCI System Research Project (Project ID: hp220120), SGI8600, at the Japan Atomic Energy Agency (JAEA) and Wisteria at the University of Tokyo with the support of the Multidisciplinary Cooperative Research Program in CCS, University of Tsukuba.

## References

1. P. Xia, C. Kim, F. Lu, T. Kanai, H. Akiyama, J. Itatani, and N. Ishii, *Opt. Express* **26**, 29393 (2018).
2. C. Yu, S. Jiang, and R. Lu, *Adv. Phys. X* **4**, 1562982 (2019).
3. Yamada, T. Otobe, D. Freeman, A. Kheifets, and K. Yabana, *Phys. Rev. B* **107**, 035132 (2023).
4. K. Yabana, T. Sugiyama, Y. Shinohara, T. Otobe, and G. F. Bertsch, *Phys. Rev. B* **85**, 045134 (2012).
5. S. Yamada and K. Yabana, *Phys. Rev. B* **103**, 155426 (2021).